UC Irvine
UC Irvine Previously Published Works

Title

Noninvasive Measurement of Ablation Crater Size and Thermal Injury after CO2 Laser in the Vocal Cord with Optical Coherence Tomography

Permalink

https://escholarship.org/uc/item/0004h998

Journal

Otolaryngology, 134(1)

ISSN

0194-5998

Authors

Torkian, Behrooz A
Guo, Shuguang
Jahng, Alexander W
et al.

Publication Date

2006

DOI

10.1016/j.otohns.2005.09.016

Copyright Information

Peer reviewed

ORIGINAL RESEARCH

Noninvasive Measurement of Ablation Crater Size and Thermal Injury After CO_2 Laser in the Vocal Cord With Optical Coherence Tomography

Behrooz A. Torkian, MD, Shuguang Guo, PhD, Alexander W. Jahng, MS, Lih-Huei L. Liaw, MS, Zhongping Chen, PhD, and Brian J.F. Wong, MD, PhD, Irvine, California

OBJECTIVE: To characterize tissue destruction after CO_2 laser-ablation of the vocal cords with the use of optical coherence tomography (OCT).

STUDY DESIGN AND SETTING: OCT was used to image fresh porcine vocal cords after laser ablation. OCT and histology estimates of the ablation crater dimensions and the depth of thermal injury were obtained.

RESULTS: The vocal cord substructures up to 2.29 mm in depth at 10 μm resolution, and the thermal disruption after laser ablation were identified by OCT. OCT and histology estimates of the lesion dimensions showed no significant differences. Crater depth is directly proportional to laser power, whereas crater width and the zone of thermal injury appear to be unrelated to laser power.

CONCLUSIONS: OCT may be used to accurately characterize the native states and the laser-induced thermal injury of laryngeal mucosa, within the inherent limitation in its depth of penetration. OCT may be a useful diagnostic and monitoring tool in an otolaryngology practice.

Optical coherence tomography (OCT) is an emerging noninvasive, noncontact, near-real time imaging modality based on low-coherence interferometry.[1-3] The technology is analogous to ultrasound, and may be adapted to endoscopes and catheters. However, rather than acoustic waves, OCT devices measure the echo-time delay and the intensity of back-reflected infrared light generated by solid state lasers or superluminescent diodes. OCT is capable of producing cross-sectional images with a resolution of 10 μm or less, with an imaging depth of 1 to 3 mm through turbid media.

In this study we compare OCT with conventional histology in the evaluation of laser injury in fresh ex vivo porcine larynges with the use of CO_2 laser irradiation. Our main goals were to determine the ability of OCT to evaluate destructive lesions created by the surgical carbon dioxide laser in the laryngeal mucosa using histology as a standard.

MATERIALS AND METHODS

Preparation and Laser Ablation

Porcine larynxes were obtained from a local packing company (Clougherty Packing Co., Vernon, CA.) within 1 hour of the animals' death. Laryngofissure was performed to expose the vocal folds. A carbon dioxide laser (Sharplan Lasers, Allendale, NJ) was used to create 10 separate lesions on the true vocal cord (TVC) mucosa. The laser beam was focused with a lens to produce a 125 μm spot size with a quartz lens (f = 150 mm). Laser pulse duration was 100 msec, and the average power ranged from 2 W to 20 W in 2 W increments. The laser beam was orthogonal to the axial plane of the TVC mucosa.

Optical Coherence Tomography Imaging

The OCT device used in this study has been previously described by Jung et al,[4] and only the general system parameters will be summarized here. The central wavelength of the OCT device used is 1310 nm and the bandwidth is 80 nm. This device provides images of 1600×510 pixels with axial resolution of 10 μm. An image 8×2.55 mm area is created. OCT images were obtained at each site immediately before and after irradiation. Each image is an optical cross-section of the vocal cord in the coronal plane. OCT data was converted to JPEG formatted images and processed using software (Photo-Paint 8, Corel, Ontario, Canada).

Histology

After OCT imaging was completed, the tissue was fixed in formaldehyde, serially dehydrated in graded ethanol baths, embedded in paraffin, and sectioned in 6 μm microsections in the coronal plane, orthogonal to the TVC surface. Sections were stained with hematoxylin and eosin (H-E).[5] Multiple thin sections were made across each specimen to allow registration with the OCT images; histologic sections spanned the entire width of each ablation crater. Digital images of the H-E stained slides were obtained with a bright-field microscope (Olympus, Melville, NY) with a digital camera, and stored as JPEG formatted images.

Micrometry

JPEG formatted OCT images and histologic photomicrographs were processed with the use of software. Photomicrographs of the specimens ablated with greater than 10 W resulted in laser craters that exceeded the length that could be captured in 1 frame. Hence, composite images of these samples were rendered with software to allow accurate measurement of the depth. Ablation crater depth, extent of thermal necrosis, and overall tissue destruction were measured with the use of the micrometry utilities in the software.

Statistics

The relationship of the power of laser to the crater dimensions and the thickness of thermal injury was determined by linear regression and Pearson's correlation for each OCT and histology. The correlation was considered to be significant at $P < 0.001$. In addition, depth estimate relationships between the 2 methodologies were similarly explored. The $P < 0.05$ was considered to be significant. Bland-Altman analysis[6] was used to determine agreement between the OCT and histology estimates of the zone of thermal injury and crater dimensions. Due to the inherent depth limitations imposed by OCT (penetration to 2.29 mm), the relationships were sought only up to 14 W for all of the above cases unless otherwise specified. The cutoff value of 14 W was determined by optimizing for correlation coefficient and agreement in depth estimates.

RESULTS

The comparison of OCT images to photomicrographs of histologic slides reveals several correlates between the sub-
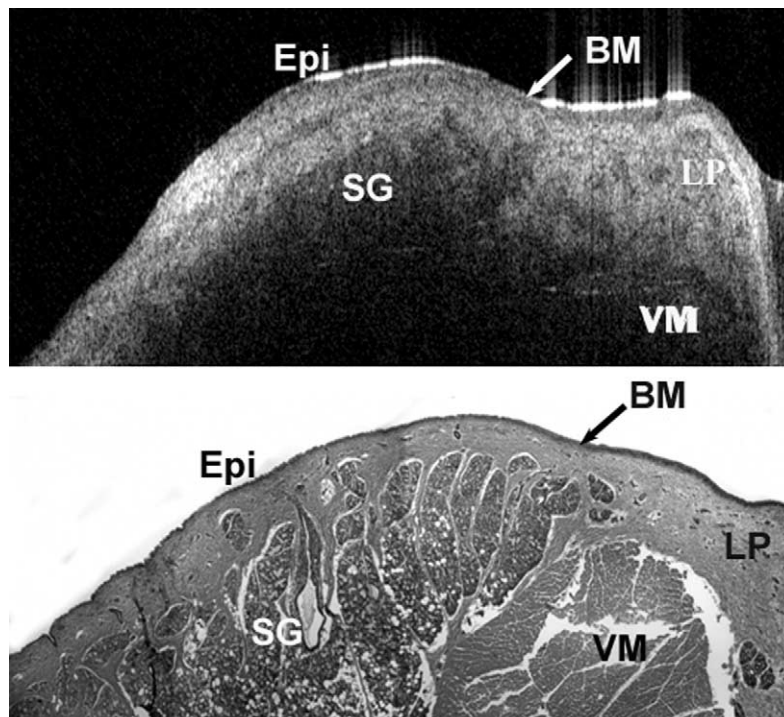
Figure 1   The structural anatomy of normal porcine vocal cords as imaged by OCT device (*top*). (*Epi*, epithelium; *BM*, basement membrane; *SG*, submucosal glands; *LP*, lamina propia; *VM*, vocalis muscle). Histology of the same specimen (*bottom*) (hemoloxylin-eosin stain).
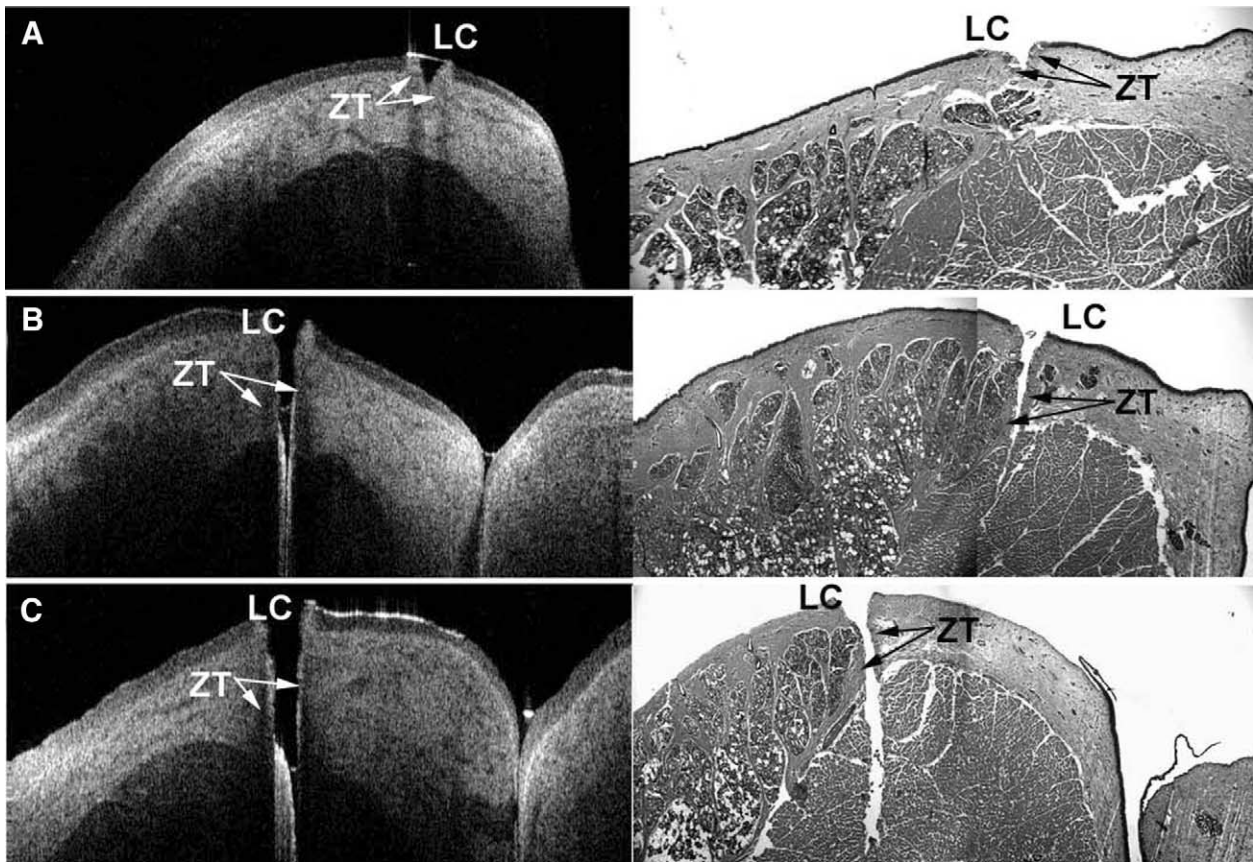
Figure 2   Porcine vocal cords after laser ablation at (**A**) 4 W, (**B**) 6 W, and (**C**) 10 W. The OCT images are shown on the left, with corresponding H-E stain on the right. (*LC*, laser-induced crater; *ZT*, zone of thermal injury.)

structural elements of the TVC mucosa as imaged in the 2 different formats. Fig 1 highlights the topography, stratification of the mucosa, submucosal glands, and vocalis muscle as seen in an OCT image and a photomicrograph of native laryngeal mucosa. The high signal intensity at the surface is thought to be due to the high differences in refractive indexes as light passes from air to the tissue layer,[3] and the immediate mucosal epithelium is present as a thin, homogeneous, low signal structure. The basement membrane is likely represented by the thin line with high signal intensity immediately beneath the epithelium. The lamina propria is depicted by low intensity heterogeneous signal suggesting the native loose, nonorganized tissue, and glandular elements that inhabit this region of the pig glottis.

OCT images of the TVC mucosa obtained immediately after laser injury are compared with the corresponding histologic sections (Fig 2). The location and overall extent of tissue destruction in relation to native tissue structures are readily apparent. The penetration of the ablation crater through the basement membrane, lamina propia, submucosal glands, or the vocalis muscle are well visualized with OCT and correlate with the histologic sections of the same region. The degree of tissue damage is easily appreciated on the OCT images. The high reflectivity at the burn surface is due to the carbonization of tissue.[7] This area correlates well with the eosinophillic dense area of homogenized collagen

at the immediate periphery of ablation craters appreciated on the photomicrographs.

The measurements of crater dimensions (depth and width) and the zone of thermal injury made with OCT and histology are summarized in Table 1A to 1C, respectively. Crater depths greater than 2.29 mm could not be measured. The intrinsic limitations of the OCT technology does not allow for accurate capture of the vocal cord anatomy beyond a certain depth of penetration. Hence, only the lesions created with up to 14 W were used for statistical analysis (see Materials and Methods, Statistics, for details).

Table 1A
Comparison of the estimates of crater depth (mm)

Power (W)	Histology	OCT
2	0.25	0.21
4	0.50	0.50
6	0.73	1.00
8	1.55	1.14
10	1.43	ND
12	1.75	1.71
14	2.15	1.71

CO_2 laser with 125 μm spot size and 100 ms pulse duration. ND, Not determined.

Table 1B
Comparison of the estimates of crater width (mm)

Power (W)	Histology	OCT
2	0.48	0.44
4	0.46	0.51
6	0.53	0.50
8	0.45	0.43
10	0.45	0.46
12	0.48	0.37
14	ND	0.29

CO_2 laser with 125 μm spot size and 100 ms pulse duration. ND, Not determined.

There is a good correlation between the laser power and crater depth as determined with both OCT (r = 0.98, $P <$ 0.001) and histology (r = 0.97, $P <$ 0.001) (Fig 3A). No significant correlation was found between the laser power and the crater width by OCT (r = -0.77, $P =$ 0.05) or histology (r = -0.19, $P =$ 0.71). No significant correlation was found between the laser power and the zone of thermal injury by either OCT (r = -0.27, $P =$ 0.56) or histology (r = -0.32, $P =$ 0.48). There is good correlation between crater depth estimates by 2 techniques (r = 0.93 and $P =$ 0.02) (Fig 3B).

The agreement between the use of OCT and histology for determining crater dimensions and the thickness of zone of injury are shown in Fig 4, and the results from Bland-Altman analysis are summarized in Table 2. The upper and lower limits of agreements, as well as mean difference, are relatively small in comparison to actual measurements, and show good agreement.

DISCUSSION

In this study, a direct comparison of OCT to conventional histologic imaging of native and laser-ablated vocal fold mucosa illustrates the ability of OCT to accurately depict

Table 1C
Comparison of the estimates of zone of thermal injury (mm)

Power (W)	Histology	OCT
2	0.13	0.11
4	0.13	0.11
6	0.13	0.14
8	0.15	0.14
10	0.15	0.11
12	0.13	0.14
14	0.10	0.07

CO_2 laser with 125 μm spot size and 100 ms pulse duration. ND, Not determined.
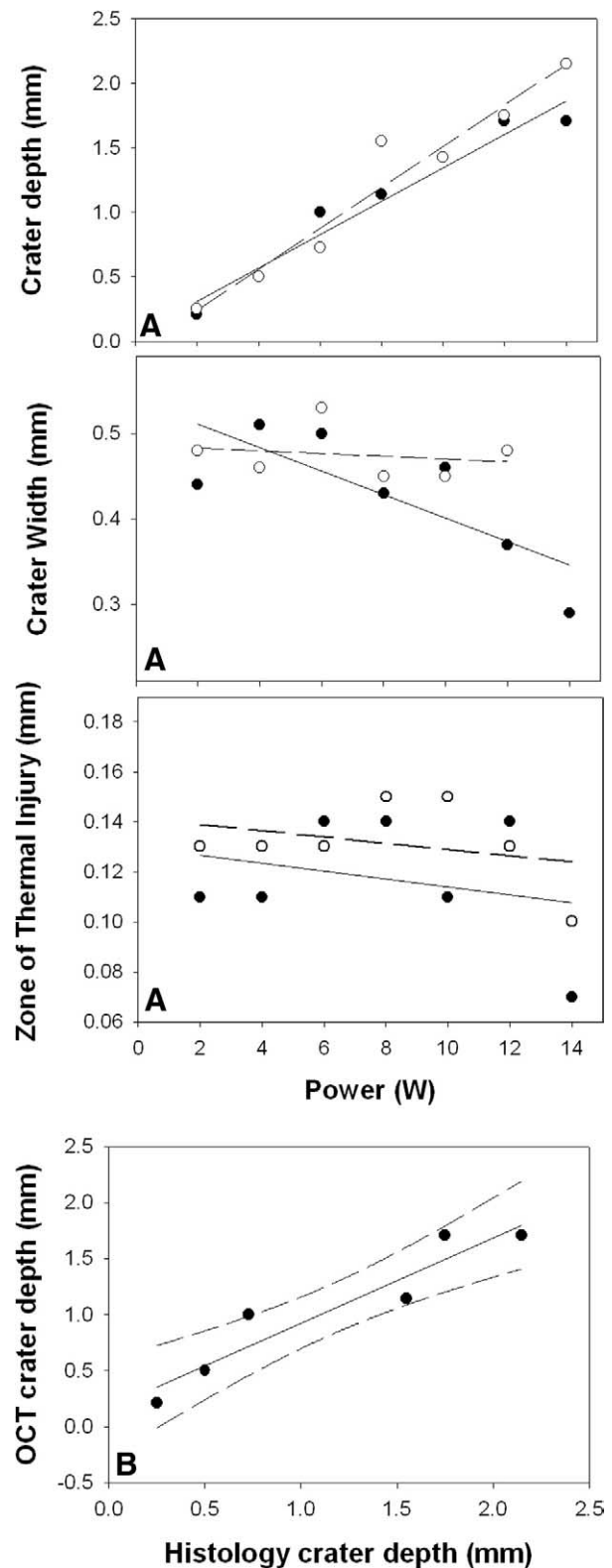
Figure 3 (**A**) Crater depth, crater width, and the zone of thermal injury as a function of power as measured by OCT (*solid circles*) or histology (*empty circles*). Linear regression lines for OCT (*solid line*) and histology (*dashed line*) are overlaid. (**B**) OCT and histology estimates of crater depth as a function of laser power. *Solid line* is the linear regression line, and *dashed lines* indicate 95% confidence intervals.
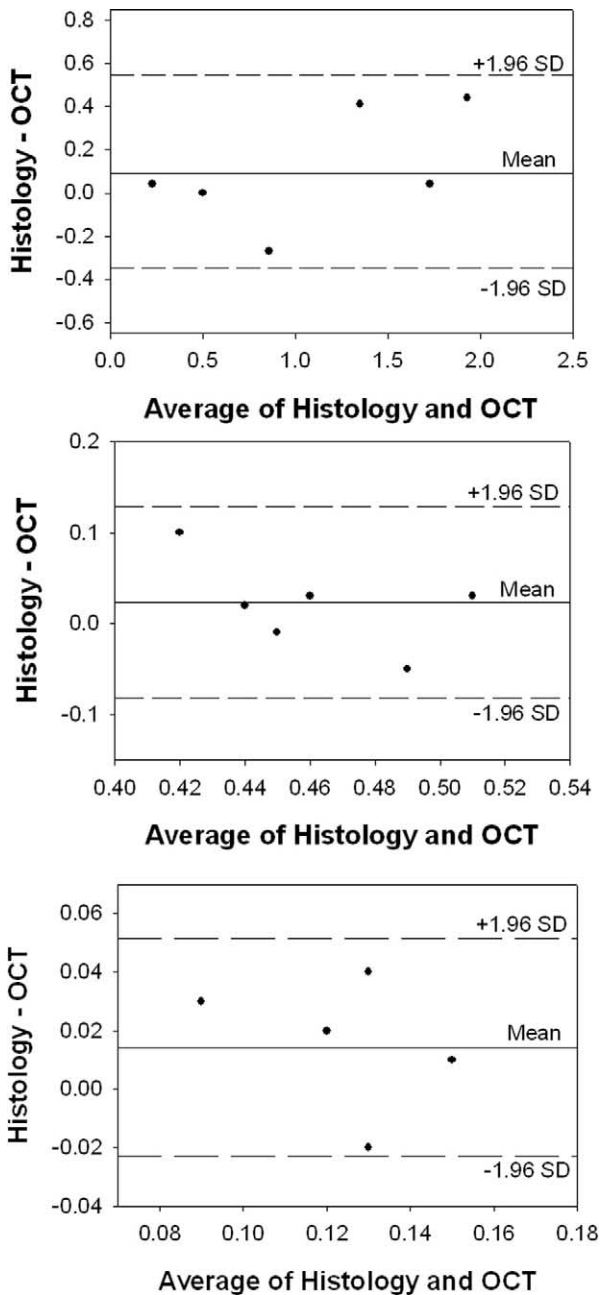
Figure 4 Agreement between OCT and histology estimates of depth (*top*), width (*middle*), and zone of injury (*bottom*) by Bland-Altman analysis. *Solid line* indicates mean difference between histology and OCT, and *dashed lines* indicate the limits of agreement (mean difference, ± 1.96 SD).

key features of native and damaged vocal fold mucosa. The ability to identify tissue stratification, substructural components, overall tissue damage, depth of injury, and zone of thermal injury on OCT images correlates well to conventional histology (Table 2, and Figs 3 and 4). In accordance with a previously published study,[5] OCT image measurements of crater depth were directly related to the power of the laser, whereas the zone of thermal injury and crater width remained relatively stable and unaffected by incremental increases in power. Measurements of tissue destruction were comparable with histologic measurements with statistical significance.

The acquisition of data in this study required capturing the entire length of a conical laser ablation crater in either a histologic section or an OCT image. Alignment of samples on the OCT stage and ensuring histologic sections through the proper plane introduces a source of error. In both OCT image acquisition and histology, it is technically challenging to obtain orthogonal sections through the exact diameter of the crater. While other authors have used a dye technique to define the site and the plane of the laser/OCT cut, others have found this technique to be unreliable.[8] In our study, the direction of the laser beam and the plane of sectioning were carefully aligned by the same researcher (BT). However, the alignment of these 2 planes is always subject to parallax and positioning errors and may account for small discrepancy in measurements made on OCT or histologic images. Second, histologic sectioning of the sample may distort the tissue section and may result in additional measurement errors. Finally, images of craters made with laser power 10 W or greater required generation of composite images from multiple images with the use of software, which introduces uncertainty due to subtle registration mismatches.

This study reiterates the inherent depth penetration limitations of OCT as the anatomy of the vocal cords could not be visualized accurately beyond 2.29 mm. This is due to intrinsic limitations produced by the combined effect of scattering and absorption of the incident photons from the low coherence source by the tissue. While the current depth of penetration provides good visualization of the basement membrane to the lamina propria and the vocalis muscle, it may limit evaluation of the depth of invasion of other more extensive pathologies. Furthermore, cellular resolution is not possible at less than 10 μm resolution with the OCT device used in this study, however our group is currently developing OCT instruments that approach 1 μm resolution.

Despite the current limitations, the potential utility of OCT in an otolaryngology–head and neck surgery practice cannot be overstated. Although limited resolution and depth of penetration may prohibit the exclusive use of OCT in the diagnosis of mucosal lesions, it may be a useful tool in

Table 2
Bland-Altman analysis of laser injury dimensions, histology versus OCT

	Limits of agreement	
	Lower limit (−1.95 SD; mm)	Upper limit (+1.95 SD; mm)
Crater depth	−0.42	0.64
Crater width	−0.08	0.13
Zone of thermal injury	−0.023	0.052

CO_2 laser power 2 to 14 W, with 125 μm spot size and 100 ms pulse duration.

conjunction with biopsies and computed tomography or magnetic resonance imaging. Office-based OCT systems may one day become a useful minimally invasive means to monitor laryngeal lesions. As an example, Bibas et al[8] have recently demonstrated that laryngeal OCT imaging in 3-dimensions is feasible, allowing for the possibility of accurate determination of gross cancer morphology. Continued advances in technology have already led to OCT machines capable of cellular resolution at 1 to 2 μm[1] and will indeed improve the diagnostic power of OCT devices.

In the operating room, using earlier generation devices with lower resolution, Shakhov et al[9] have demonstrated that OCT provided a more objective estimate of the tumor margins than that observed with traditional endoscopic and microscopic techniques. They observed that surgeons took extended margins of excision by an average of 1 to 3 mm using OCT guidance. Similarly, a method of feedback-controlled laser excision is described by Boppart et al,[7] where laser irradiation was terminated before tissue ejection and membrane rupture as seen on a near-real time OCT system.[7]

Our results support the continued investigation of OCT as a modality to aid diagnosis and the medical and surgical management of laryngeal lesions. Based on these observations, high-resolution OCT imaging may also eventually prove useful in the operating room as tool to determine the adequacy of surgical margins, to provide exquisite control of excision, and to limit thermal injury on the surrounding tissues by providing real-time data on the thermal trauma states of the surrounding tissues.

CONCLUSION

OCT is an emerging imaging modality with actively increasing resolution and functionality. This study demonstrates that OCT is capable of providing anatomic images of the structure of the normal and laser ablated vocal cords within the confines of its limited tissue depth penetration. The boundaries and dimensions of both tissue substructures and ablation injury can be measured with OCT. OCT images were also able to accurately capture the unique qualities of the thermal injury generated by the carbon dioxide laser: homogenization and carbonization of the tissue. These results support the continued investigation of OCT as a diagnostic and surgical device in the field of otolaryngology.

REFERENCES

1. Fujimoto JG. Optical coherence tomography for ultrahigh resolution in vivo imaging. Nat Biotechnol 2003;21(11):1361–7.
2. Tadrous PJ. Methods for imaging the structure and function of living tissues and cells: 1. Optical coherence tomography. J Pathol 2000; 191(2):115–9.
3. Welzel J. Optical coherence tomography in dermatology: a review. Skin Res Technol 2001;7(1):1–9.
4. Jung W, Zhang J, Mina-Araghi R, et al. Feasibility study of normal and septic tracheal imaging using optical coherence tomography. Lasers Surg Med 2004;35(2):121–7.
5. Wong BJ, Si MS, Cho C, et al. XeCl laser surgery of the vocal cords: a histologic comparison with CO2 laser in a porcine model. Otolaryngol Head Neck Surg 1998;118(3 pt 1):371–5.
6. Bland JM, Altman DG. Statistical method for assessing agreement between two methods of clinical measurement. Lancet 1986;1(8476): 307–10.
7. Boppart SA, Herrmann J, Pitris C, et al. High resolution optical coherence tomography-guided laser ablation of surgical tissue. J Surg Res 1999;82(2):275–84.
8. Bibas AG, Podoleanu AG, Cucu RG, et al. 3-D optical coherence tomography of the laryngeal mucosa. Clin Otolaryngol 2004;29(6): 713–20.
9. Shakhov AV, Terentjeva AB, Kamensky VA, et al. Optical coherence tomography monitoring for laser surgery of laryngeal carcinoma. J Surg Oncol 2001;77(4):253–8.